Sains Malaysiana 39(3)(2010): 423–433

A Surface Potential Study of Ion-Uptake by 5,11,17,23-Tetra-*Tert*-Butyl-25,27-Diethoxycarbonyl Methyleneoxy-26,28,Dihydroxycalix[4]Arene and 5,17-(3-Nitrobenzylideneamino)-11,23-Di-*Tert*-Butyl-25,27- Diethoxycarbonyl Methyleneoxy-26,28-Dihydroxycalix[4]Arene Langmuir Blodgett (LB) Monolayers

(Kajian Potensi Permukaan Bagi Angkutan-Ion oleh Satu Lapisan Langmuir Blodgett (LB) 5,11,17,23-tetra-tert-butil-25,27-dietoksikarbonil metileneoksi-26,28,dihidroksikaliks[4]aren dan 5,17-(3-nitrobenilideneamino) -11,23-di-tert-butil-25,27- dietoksikarbonil metileneoksi-26,28-dihidroksikaliks[4]aren)

F.L. Supian, T.H. Richardson*, M. Deasy, F. Kelleher, J.P. Ward & V. Mckee

ABSTRACT

*A study of surface pressure - area (Π-A) isotherms, surface potential (ΔV) and effective dipole moment ($\mu_\perp$) of two calix[4] arenes, 5,11,17,23-tetra-tert-butyl-25,27-diethoxycarbonyl methyleneoxy-26,28,dihydroxycalix[4]arene (calixarene **I**) and 5,17-(3-nitrobenzylideneamino)-11,23-di-tert-butyl-25,27-diethoxycarbonyl methyleneoxy-26,28-dihydroxycalix[4] arene (calixarene **II**) LB films which have the same lower rim but different upper rim has been carried out. This work used a NIMA Surface Potential (S-POT) sensor attached to an LB trough. Space filling model or Corey, Pauling and Koltun (CPK) precision molecular models have been used to estimate the size and the flexibility of both calix[4]arenes, which has been confirmed by X-Ray analysis in one case. The Π-A-isotherms confirmed that both of the calix[4]arenes form a monolayer film and the orientations of the plane of the calix ring are parallel with the air-water interface. The value of limiting area, (A_{lim}) increases as a result of adding Fe^{3+} salt in the water subphase. For **I**, the value increases from 1.28 nm^2 to 1.44 nm^2 while for **II**, it increases from 1.70 nm^2 to 1.86 nm^2. ΔV measurements were performed on a water subphase containing Fe^{3+} salt in the concentration range 0 – 1.25 × 10^{-1} mM. ΔV of the compressed monolayer films increased with increasing Fe^{3+} concentration indicating the presence of Fe^{3+} salt bound within the calix[4]arenes. Using the ΔV values, the effective dipole moment has been found using the Helmholtz equation.*

Keywords: Π-A isotherm, calix[4]arenes, effective dipole moment; LB; surface potential

ABSTRAK

*Tekanan permukaan–kawasan isoterma (Π-A), potensi permukaan (ΔV) dan momen dwikutub berkesan ($\mu_\perp$) bagi dua filem LB kaliks[4]arene, 5,11,17,23-tetra-tert-butil-25,27-dietoksikarbonil metileneoksi-26,28,dihdroksikaliks[4] aren (kaliksaren **I**) dan 5,17-(3-nitrobenzilideneamino)-11,23-di-tert-butil-25,27-dietoksikarbonil metileneoksi-26,28-dihidroksikaliks[4]aren (kaliksaren **II**) yang mempunyai struktur bawah yang sama tetapi struktur atas yang berbeza telah dikaji. Kajian menggunakan sensor potensi permukaan NIMA (S-POT) pada alat LB. Model ruang penuh atau model kepersisan molekul Corey, Pauling dan Koltun (CPK) telah digunakan untuk menganggar saiz dan kefleksibelan bagi kedua-dua kaliks[4]aren, dan dalam satu kes telah disahkan dengan analisis sinar-X. Isoterma Π-A mengesahkan bahawa kedua-dua kaliks[4]aren membentuk satu lapisan filem dan orientasi bagi cincin kaliks adalah selari dengan permukaan udara-air. Nilai bagi kawasan terhad (A_{lim}) bertambah apabila ditambah Fe^{3+} di dalam air. Bagi **I**, nilai bertambah daripada 1.28 nm^2 ke 1.44 nm^2 manakala bagi **II**, ia bertambah daripada 1.70 nm^2 ke 1.86 nm^2. Pengukuran ΔV dilakukan pada sub-fasa air yang mengandungi garam Fe^{3+} pada julat ketumpatan 0 – 1.25 × 10^{-1} mM. Pertambahan ΔV filem satu lapisan mampat dengan pertambahan kepekatan Fe^{3+} menandakan kehadiran garam Fe^{3+} bergabung dengan kaliks[4]arene. Menggunakan nilai-nilai ΔV, momen dwikutub berkesan telah diperolehi dengan menggunakan persamaan Helmholtz.*

Kata kunci: Isoterma Π-A; kaliks[4]aren; LB; momen dwikutub berkesan; potensi permukaan

Introduction

Basket-shaped macromolecules known as calixarenes have proved popular building blocks for the development of highly specific synthetic receptors particularly for ionic guest species (Gutsche 1998; Casnati & Ungaro 2000).

They are attractive candidates for use in novel sensing materials since their properties are often modified via such binding interactions. Calix[*n*]arenes are macrocyclic compounds in which phenolic units are linked via methylene bridging groups at their *ortho* positions.

The spectacular development of these well defined macromolecular systems in recent years is related to the ease with which the upper (aryl) and lower (phenolic) rims have been modified in a stereocontrolled and regiocontrolled manner, coupled with the wide range of cationic and neutral and guests they have been found to bind. The smallest in the series is where four phenolic units make up the macrocyclic backbone (n = 4). This offers a highly rigid platform on which to attach functional groups with potential to act as pre-organised binding sites for selective complexation, hence they have been widely studied in the field of molecular recognition, transportation and separation (Creaven et al. 2009). Langmuir-Blodgett (LB) films formed by calixarenes can be used to explore these functions.

The chemical structures of the two calix[4]arenes used in this study are shown in Figure 1. They are similar in cavity size and conformation, but differ in their substituents at the wider or upper rim. **I** is the known distal di-derivatised calix[4]arene compound bearing terminal ester groups at the narrow lower rim of the calixarene scaffold, where binding in solution normally occurs with alkali metal guests (Collins & McKervey 1989).

The relatively rigid cone structure at this narrow rim often precludes strong binding to larger metal ions. The wider (upper rim) bears lipophilic *tert*-butyl groups with no ionophoric activity. **II** is a new calix[4]arene derivative synthesied by this group with the same functional groups at the lower rim, but with more diverse binding sites at the wider rim, to facilitate binding to the larger transition metals. Fe^{3+} is a physiologically important metal cation and plays a catalytic role in many processes such as oxygen metabolism and electron transfer (Aisen et al. 1999; Eisenstein 2000). A deficiency or excess can contribute to serious disease (Andrews & Engl 1999; Touati 2000; Cairo & Pietrangelo 2000; Beutler et al. 2001) hence detection of Fe^{3+} is of great importance. There have been only a few Fe^{3+} chemosensors reported to date (Zhang et al. 2009; Zhang & Fan 2009).

Calix[4]arenes have been successfully employed in ion selective electrodes (Cadogan et al. 1989; O'Connor et al. 1992; Diamond & McKervey 1996; Zeng et al. 2000; Lu et al. 2004; Lu et al. 2002; Lu et al. 2003). Difficulties associated with electrode modification can result in lower sensitivities being achieved, than is required for the determination of low levels of ionic species present in some real samples (Zhang et al. 2009).

In recent years, there has been an increase in the level of interest in the generation of ultrathin organic films, encapsulating ionophoric macromolecules, using techniques such as Langmuir-Blodgett (LB), as a way of overcoming such problems (Wang et al. 2009; Nabok et al. 1997).

The advantage of using the LB technique lies in the fact that sequential layers of ultrathin films can be formed, with controlled thickness and order on the molecular scale (Fanucci et al. 2001; Wu et al. 2001).

Calixarenes form stable Langmuir films at air-water interface due to their amphiphilic structure (Lonetti *et al*. 2005). A way to understand the behaviour of Langmuir monolayers at the air-water interface is through the surface potential measurement (ΔV) (Taylor & Bayes 1999). Based on the ΔV values, the effective dipole moment (μ_1) of molecules at the interface can be calculated using the Helmholtz equation (Korchowiec et al. 2007). In this work, determination of the Langmuir properties of two calixarenes containing very different upper rims (one a conjugated push-pull electron system, the other a small-dipole system) is reported and the associated changes resulting from the addition of an Fe^{3+} analyte.

The synthesis of double-armed calixarenes with ionophoric ligating groups is well known, both with simple alkyl halides, RX or those with further functionality, for example XCH_2COOR. Hence, I was prepared in three steps as follows. *p-tert*-Butylcalix[8]arene (cyclic octamer) was first prepared by the modified Munch procedure (Gutsche et al. 1981; Munch & Gutsche 1990) from *p-tert*-butylphenol and paraformaldehyde in the presence

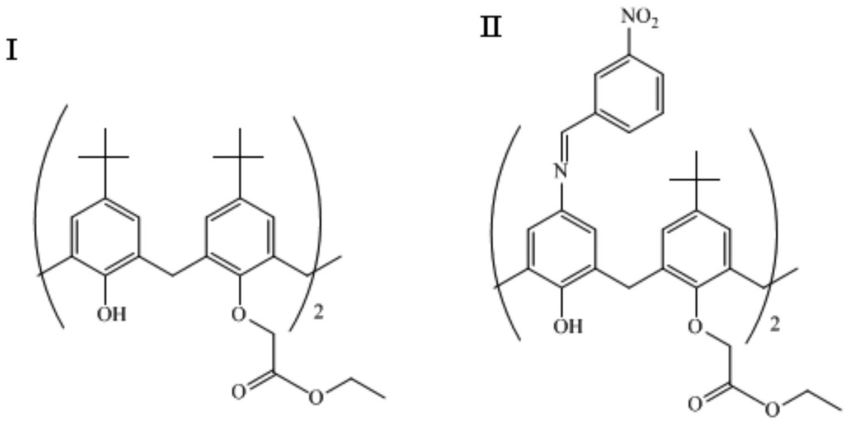

FIGURE 1. Compound **I**: 5,11,17,23-tetra-*tert*-butyl-25,27-diethoxycarbonyl methyleneoxy-26,28, dihydroxycalix[4]arene; and Compound **II**: 5,17-(34-nitrobenzylideneamino)-11,23-di-*tert*-butyl-25,27- diethoxycarbonyl methyleneoxy-26,28-dihydroxycalix[4]arene

of KOH and was isolated as a white powder, in 70% yield. This was then subjected to molecular mitosis (Gutsche et al. 1985; Schmitt et al. 1997) to form *p-tert*-butylcalix[4] arene (cyclic tetramer). Sodium hydroxide was the base of choice due to the template effect between the cavity size of the tetramer and the size of the Na^+ cation, which induced formation of the tetramer in a 71% yield. The reaction of *p-tert*-butylcalix[4]arene with ethyl bromoacetate, under conventional conditions for AC alkylation (K_2CO_3 as base in acetonitrile as solvent) (Arnaud-Neu et al. 1989) resulted in the expected A,C-dialkyl derivative I with terminal ester groups.

The upper rim derived Calix-Schiff II was synthesized from I by the synthetic route shown in Figure 2. The distal di-derivatised calixarene I was subjected to nitro-dealkyation, according to the literature procedure by W. Verboom et al. 1992.

Reduction of the nitro calix[4]arene **IA** to the calix[4] arene diamine **IB** was achieved by hydrogenation, at 2 atm. of pressure, in ethanol in the presence of Raney-Nickel in

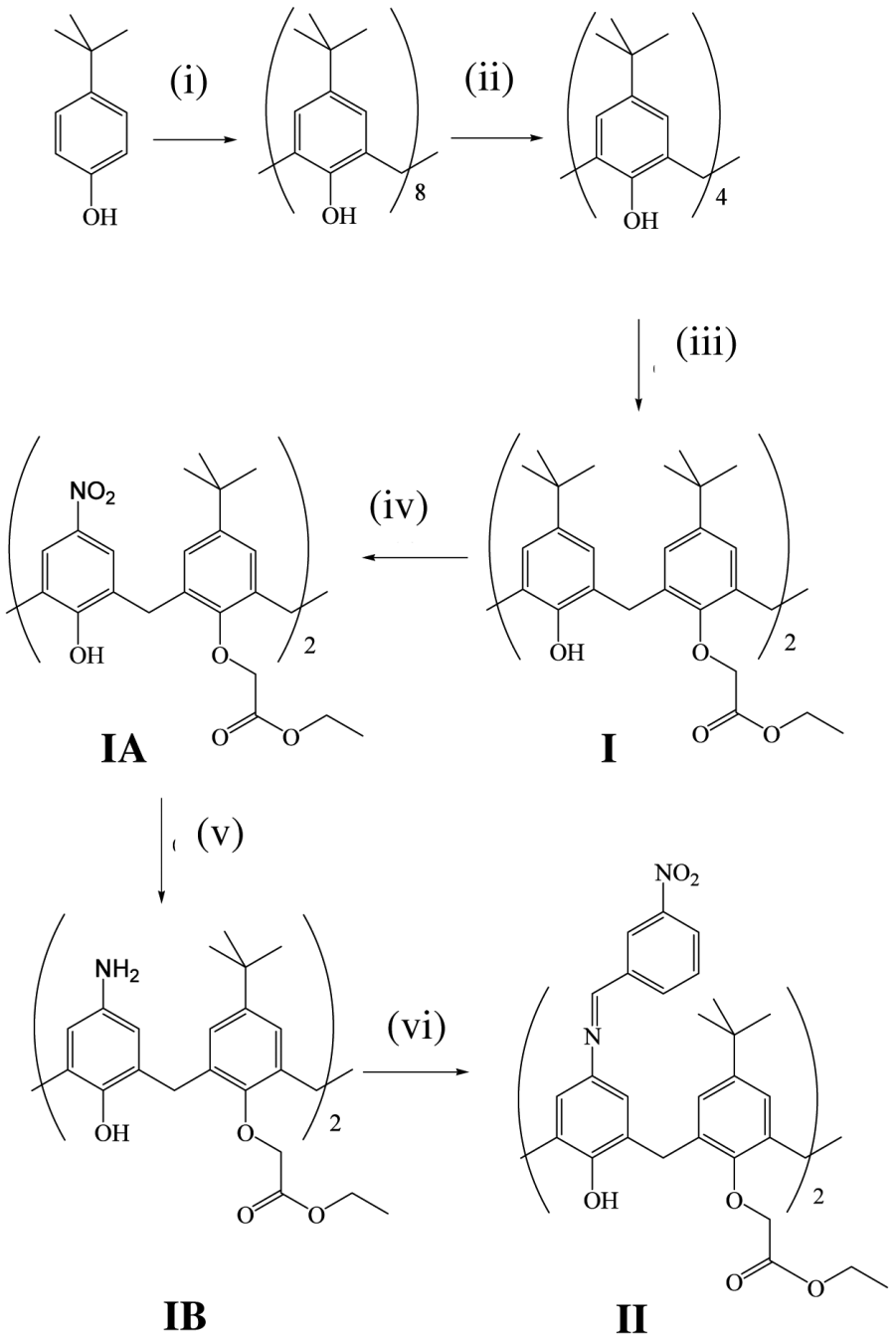

FIGURE 2. Reaction Conditions: (i) HCHO, KOH, xylene; (ii) NaOH, Ph_2O; (iii) $BrCH_2COOEt$, K_2CO_3, CH_3CN; (iv) HNO_3, CH_3COOH, CH_2Cl_2; (v) H_2 (2 atm.), Ra/Ni, EtOH; (vi) 3-nitrobenzaldehyde, EtOH

almost quantitative yield (99%). The ^{1}H NMR spectrum displayed a broad singlet at 6.30 ppm, which exchanged with D_2O, for the NH_2 group at the upper rim. An upfield shift was noted for the aromatic protons which resonated at 7.01 ppm and 6.95 ppm. The *tert*-butyl protons also shifted downfield to 1.24 ppm. A quartet at 4.29 ppm and triplet at 1.32 ppm were observed for the ester protons. The ^{13}C NMR spectrum showed an upfield shift for the ArC_q-OH to 151.7 ppm and peaks for the ester CH_2 and ester CH_3 were observed at 61.2 ppm and 14.2 ppm, respectively. The IR spectrum showed an absorbance for the NH_2 and phenolic OH at 3310 cm^{-1} while the ester carbonyl group absorbed at 1746 cm^{-1}. No signals were apparent for the NO_2 group indicating successful reduction to the diamine.

The attachment of N-ligating groups through imine bond formation has been successful at the upper and lower rim of calixarenes. This has resulted in the formation of calixarene-Schiff base receptors which have shown potential for cation recognition, particularly with transition metals (Creaven et al. 2008).

Therefore the calixarene diamine **IB** was heated to reflux temperature in ethanol with a 5 molar excess of *3*-nitrobenzaldehyde. A yellow precipitate was isolated after cooling which was recrystallised from chloroform/methanol to give pure Schiff base derivatised calixarene **II** in a 67% yield. The ^{1}H NMR of IB no longer displayed a signal for the calixarene NH_2, indicating reaction had occurred with the aldehyde. No signal appeared for the aldehyde while a sharp singlet resonated at 8.46 ppm for the imine CH indicating successful formation of the Schiff base. A series of multiplets, a result of coupling between the aromatic protons on the nitrobenzene ring, were observed from 8.67 ppm to 7.58 ppm. The phenolic OH resonated as a singlet at 7.82 ppm while the calixarene aromatic protons appeared as two singlets at 7.04 ppm and 7.00 ppm. A quartet at 4.30 ppm and triplet at 1.38 – 1.34 ppm were observed for the ester CH_2 and CH_3 respectively. The *tert*-butyl protons shifted upfield to 1.12 ppm as a result of a shielding effect upon the loss of the NO_2 group on the opposite calixarene rings. A new peak was also observed for the imine CH at 159.7 ppm in the ^{13}C NMR spectrum of **II**. The *tert*-butyl $C(CH_3)_3$ and $C(CH_3)_3$ signals shifted upfield to 141.1 ppm and 30.9 ppm respectively. The nitrophenyl ArC_q signals were observed at 147.6 ppm (ArC_q-NO_2) and 143.6 ppm while the nitrophenyl ArCH signals appeared between 134.2 ppm and 125.4 ppm. The ester CH_2 and CH_3 signals were observed at 62.3 ppm and 14.1 ppm, while the ester C=O resonated at 168.4 ppm, indicating that no reaction had taken place at the lower rim.

Elemental analysis found for **II** was in agreement with $C_{58}H_{60}N_4O_{12}.H_2O$ with a signal for water also being observed in the ^{1}H NMR spectrum of the compound at 1.57 ppm. The inclusion of solvent is a common occurrence. The mass spectral analysis for [M+1] **II** was calculated as 1005.4, which was in agreement with the observed value.

Experimental Procedures

Calixarene synthesis and compound data

Preparation of 5,11,17,23-tetra-tert-butyl-25,27-diethoxycarbonyl methyleneoxy-26,28,dihydroxycalix[4] arene [I] The calixarene diester derivative (I) was prepared in 81% yield following a procedure similar to that described by McKervey et al., m.p.: 172 – 174ºC (lit.[19] 182 – 184°C); R_f: 0.21 (70% DCM/petroleum ether); υ_{max}/cm^{-1} *(KBr)*: 3427 (polymeric OH str.), 2962, 2902, 2864 (C-H str.), 1751 (C=O str); δ_H/ppm (300 MHz, $CDCl_3$): 7.07 (2H, s, phenolic OH), 7.02 (4H, s, ArCH), 6.82 (4H, s, ArCH), 4.72 (4H, s, -O-C<u>H</u>$_2$-CO_2CH_3), 4.45 (4H, d, Ar-CH_2-Ar, *J* = 12.0 Hz), 4.30 (4H, q, C<u>H</u>$_2$$CH_3$, *J* = 7.0 Hz), 3.32 (4H, d, methylene, *J* = 12.0 Hz), 1.33 (6H, t, CH_2C<u>H</u>$_3$, *J* = 7.0 Hz), 1.30 & 1.26 (2 x 18H, s, *tert*-butyl); δ_C/ppm (75 MHz, $CDCl_3$): 169.2 (ester C=O), 150.7 (ArC_q-OH), 150.3 (ArC_q-OR), 147.1, 141.5 (ArC_q-*tert*-butyl), 132.5, 128.0 (ArC_q), 125.7, 125.1 (ArCH), 72.4 (Ar-O-<u>C</u>H$_2$), 61.2 (ester -<u>C</u>H$_2$$CH_3$), 33.9, 33.7 ($C_q$ *tert*-butyl), 31.8 (Ar-<u>C</u>H$_2$-Ar), 31.6, 31.0 (*tert*-butyl CH_3), 14.2 (ester -CH_2<u>C</u>H$_3$).

Preparation of 5,17-dinitro-11,23-di-tert-butyl-25,27-diethoxycarbonyl methyleneoxy-26,28-dihydroxycalix[4] arene [IA] Nitro de-alkylation of the diethyl ester calixarene **I** was achieved following the literature procedure (Eisenstein 2000) using nitric acid in a mixture of acetic acid and dichloromethane. Recrystallisation from methanol afforded a yellow solid (4.32 g, 21%). M.p.: 197-199 ºC (lit.[20] 198-200ºC); R_f: 0.42 (70% DCM/Pet. ether); υ_{max}/cm^{-1} *(KBr)*: 3289 (phenolic OH), 2967; 2868 (aliphatic CH), 1727 (C=O), 1510; 1336 (NO_2); δ_H/ppm (300 MHz, $CDCl_3$): 8.94 (s, 2H, phenolic OH), 7.96 (s, 4H, ArCH), 7.03 (s, 4H, ArCH), 4.72 (s, 4H, -OCH_2CO), 4.51 (d, 4H, Ar-CH_2-Ar), 4.32 (q, 4H, ester CH_2), 3.44 (d, 4H, Ar-CH_2-Ar), 1.36 (t, 6H, ester CH_3), 1.09 (s, 18H, *tert*-butyl); δ_C/ppm (75 MHz, $CDCl_3$): 168.6 (C=O), 158.8 (C_qAr-OH), 151.8 (ArC_q-OR), 144.8 (C_qAr-*tert*-butyl), 141.8 (C_qAr-NO_2), 131.1 (ArC_q), 128.9 (ArC_q), 126.8, 125.4 (ArCH), 73.5 (-O<u>C</u>H$_2$CO), 60.8 (ester CH_2), 33.9 (C_q-*tert*-butyl), 31.7 (Ar-<u>C</u>H$_2$-Ar), 29.9 (*tert*-butyl CH_3), 14.0 (ester CH_3).

Preparation of 5,17-diamino-11,23-di-tert-butyl-25,27-diethoxycarbonyl methyleneoxy -26,28-dihydroxycalix[4] arene [IB] To a suspension of dinitro calixarene **IA** (2 g, 2.4 mmol) in ethanol (200 mL) was added a catalytic amount of Raney-Nickel. The mixture was placed on a hydrogenator for 2 hours (2 atm) then filtered through a bed of celite. The solvent was removed *in vacuo* to leave compound IB as a pink solid (1.97 g, 99%), m.p.: 175 – 177ºC; R_f = 0.75 (DCM/Pet. Ether); υ_{max}/cm^{-1} *(KBr)*: 3310 (phenolic OH & NH), 1746 (C=O); δ_H/ppm (300 MHz, $CDCl_3$): 7.12 (s, 2H, phenolic OH), 7.01 (s, 4H, ArCH), 6.95 (s, 4H, ArCH), 6.30 (s, 4H, NH_2), 4.82 (s, 4H, -OCH_2CO), 4.52 (d, 4H, Ar-CH_2-Ar), 4.29 (q,

4H, -C<u>H</u>$_2$CH$_3$), 3.21 (d, 4H, Ar-CH$_2$-Ar), 1.32 (t, 6H, -CH$_2$C<u>H</u>$_3$), 1.24 (s, 18H, *tert*-butyl); δ_C/ppm (75 MHz, $CDCl_3$): 169.9 (C=O), 151.7 (C$_q$Ar-OH), 147.2(ArC$_q$-OR), 149.3 (C$_q$Ar-*tert*-butyl), 141.8 (C$_q$Ar-NO$_2$), 133.5 (ArC$_q$), 130.7 (ArC$_q$), 126.0, 116.2 (ArCH), 72.0 (-O<u>C</u>H$_2$CO), 61.2 (ester CH$_2$), 34.2 (*tert*-butyl CH$_3$), 32.3 (Ar-<u>C</u>H$_2$-Ar), 29.7 (*tert*-butyl CH$_3$), 14.2 (ester CH$_3$).

*Preparation of 5,17-(3-nitrobenzylideneamino)-11,23-di-tert-butyl-25,27- diethoxycarbonyl methyleneoxy-26,28-dihydroxycalix[4]arene [**II**]* To a solution of calixarene diamine **IB** (1.0 g, 1.2 mmol) in ethanol (75 mL) was added *m*-nitrobenzaldehye (1.0 g, 6 mmol) and the solution was heated at reflux temperature for 16 hours. After cooling, the solid residue was recovered by vacuum filtration and recrystallised from chloroform/methanol to give a yellow solid (0.80 g, 67%). M.p.: 242 – 244ºC; R_f: 0.48 (30% EtOAc/Pet. Ether); $C_{58}H_{60}N_4O_{12}.H_2O$ requires C, 68.09%, H, 6.11%, N, 5.48%; found C, 68.09% H, 6.11% N, 5.48%; ES$^+$ for $C_{58}H_{60}N_4O_{12}$, expected [M+H]: 1005.4, observed [M+1]: 1005.4; υ_{max}/cm^{-1} *(KBr)*: 3401 (phenolic OH), 2953; 2866 (aliphatic CH), 1739 (C=O), 1624 (C=N), 1526; 1349 (NO$_2$); δ_H/ppm (300 MHz, $CDCl_3$): 8.67 (s, 2H, -N=C-C$_q$-C<u>H</u>-C$_q$-NO$_2$), 8.46 (s, 2H, imine CH), 8.27 – 8.25 (m, 2H, NO$_2$-C$_q$-<u>C</u>H-CH-CH-C$_q$), 8.17 – 8.15 (m, 2H, NO$_2$-C$_q$-CH-CH-C<u>H</u>-C$_q$), 7.82 (s, 2H, phenolic OH), 7.63 – 7.58 (t, 2H, NO$_2$-C$_q$-CH-C<u>H</u>-CH-C$_q$), 7.04 (s, 4H, ArCH (calix)), 7.00 (s, 4H, ArCH (calix)), 4.82 (s, 4H, ArC$_q$-O-C<u>H</u>$_2$-O-), 4.58 – 4.53 (d, 4H, Ar-CH$_2$-Ar), 4.38 – 4.30 (q, 4H, ester CH$_2$), 3.45 – 3.41 (d, 4H, Ar-CH$_2$-Ar), 1.38 – 1.34 (t, 6H, ester CH$_3$), 1.12 (s, 18H, *tert*-butyl); δ_C/ppm (75 MHz, $CDCl_3$): 168.4 (C=O), 159.7 (imine CH), 150.9 (ArC$_q$-OH), 149.7 (ArC$_q$-OR), 147.6 (ArC$_q$-NO$_2$), 143.6 (ArC$_q$-N=C-), 141.1 (ArCq-*tert*-butyl), 134.2, 130.1, 126.7, 125.4 (ArCH (nitrobenzene)), 132.2, 127.1 (ArC$_q$ (calix)), 127.4, 124.9 (ArCH (calix)), 73.8 (ArC$_q$-O<u>C</u>H$_2$-O-), 62.3 (ester CH$_2$), 34.2 (C$_q$-*tert*-butyl), 33.8 (Ar-<u>C</u>H$_2$-Ar), 30.9 (*tert*-butyl CH$_3$), 14.1 (ester CH$_3$).

X-RAY EXPERIMENT

Diffraction data for Calix-Schiff **II** were collected at 150(2)K on a Bruker Apex **II** CCD diffractometer. The structure was solved by direct methods (Burla *et al*. 2005) and refined on F^2 using all the reflections (Sheldrick 2008). All the non-hydrogen atoms were refined using anisotropic atomic displacement parameters and hydrogen atoms were inserted at calculated positions using a riding model. $C_{58}H_{60}N_4O_{12}$, monoclinic, C_2, a = 25.174(3), b = 10.8910(15), c = 10.0060(14) Å, β = 112.315(2)º, V = 2537.9(6) Å^3, T = 150(2)K, λ = 0.71073 Å, Z = 2, 10963 reflections measured, 2637 unique (R_{int} = 0.0391), $wR2$ = 0.1544 (all data), $R1$ = 0.0542 ($I > 2\sigma(I\upsilon)$).

CPK PRECISION MOLECULAR MODELS

The CPK (Corey, Pauling and Koltun) Models, also known as space filling models, exhibit accurately scaled values corresponding to the atomic size, bond angle (accuracy of 0^{0}30') and bond length while the surface usually represents the van der Waals radius (accuracy of ± 0.003 nm) of the individual atoms.

LANGMUIR BLODGETT (LB) STUDIES

The salt iron (III) perchlorate hydrate ($Fe(ClO_4)_3$ xH_2O) was purchased from Sigma Aldrich and was dissolved in the subphase of highly purified (Elga Purelab Option) water to a concentration of ranging from 1.25 × 10^{-2} mM and 12.25 × 10^{-2} mM. The solution of both materials, concentration of 0.2 mg/ml was prepared by dissolving 2mg of **I** and **II** powder in 10 ml of Chloroform ($CHCl_3$). The experiments were divided into four procedures; (1) CPK precision molecular models (2) π-A- isotherms, (3) Surface potential measurements and (4) Effective dipole moment.

Π-A- isotherms The Π-A isotherms and surface potential measurements were recorded on a NIMA Langmuir trough (Type: 611; Serial no: 014) using a pure water subphase. A quantity of 50µl of the solution was spread onto the water surface, initially using pure water subphase and later with Fe^{3+} salts for 12 different concentrations over the range 1.25 × 10^{-2} mM to 12.25 × 10^{-2} mM. A compression speed of 100 cm^2 min^{-1} (maximum trough area = 535 cm^2) was used.

SURFACE POTENTIAL AND EFFECTIVE DIPOLE MOMENT MEASUREMENTS

The NIMA surface potential probe has a precision of ± 1mV together with the LB trough (Figure 3). It connects directly to the existing NIMA Interface Unit. While the LB software measures the surface pressure at the air-water interface, the ΔV sensor measures the potential difference above and below the film. Changes in surface pressure are only detected once a closely packed monolayer begins to form, whereas ΔV often increases as soon as the molecules are spread onto the water surface. During compression, as the orientation of the molecules change, the alignment of molecular dipoles causes a large change in the surface potential (NIMA 2009).

A net potential or Volta potential arises when the molecules are aligned at a surface and a double layer of charges exists. ΔV is hence the change in the Volta potential between the clean water surface and the monolayer coated surface. From the ΔV, the molecular orientation and dipole per molecule can be calculated. (Langmuir Films or Insoluble Monolayers at the Air Water Interface 2009).

From the ΔV values, $\mu_\perp$ of molecules at the interface can be calculated using either equation (1) or (2). Equation (1) is from the Helmholtz equation:

$$\Delta V = \frac{\mu_\perp}{\varepsilon_0 \varepsilon A} \qquad (1)$$

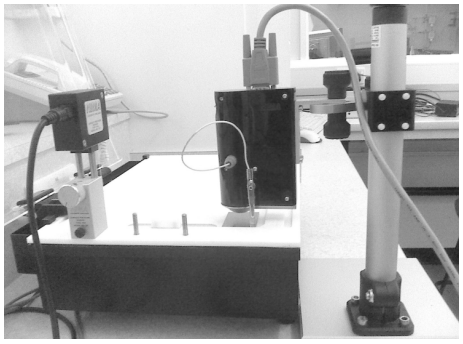

FIGURE 3. NIMA surface potential (S-POT) sensor attached to LB trough

where A is the area per molecule, ε_o is the vacuum permittivity (8.854×10^{-12} C^2 N^{-1} m^{-2}), ε is the relative permittivity of the monolayer (here, it is assumed to be 1) (Korchowiec et al. 2007).

The same values also can be obtained from equation (2):

$$\mu_{\perp} = \Delta V A(2.65 \times 10\text{-}2). \quad (2)$$

where A is the area permolecule in Å^2, and 2.65×10^{-2} C m^{-1} V^{-1} is a constant arising from converting the dipole moment into Debye units ((1 D = 3.33564×10^{-30} C m) Osvaldo et al. 1997).

RESULTS AND DISCUSSIONS

X-RAY RESULTS

Crystals of Calix-Schiff **II**, suitable for an X-ray diffraction study, were obtained from chloroform/methanol. The X-ray crystal structure of **II** is shown below (Figure 4).

The molecule lies on a 2-fold axis and adopts a distorted cone conformation in the solid state. The conformation of **II** is defined by the angles which the aromatic rings make with the plane of the four methylene carbon atoms which link them, viz 75.59(8)º and 43.33(9) º for the rings carrying the Schiff base and the *tert*-butyl groups, respectively. There is an intramolecular O-H···O hydrogen bond between the the phenolic O-H group and a proximal ethereal oxygen (O3-H3···O5 0.2692(4) nm. The molecules are stacked one inside the other, with the stacks running parallel to the b axis as shown in Figure 5.

CPK PRECISION MOLECULAR MODELS

CPK modelling reveals a projected area per molecule for **I** and **II** ranging from 1.21- 1.96 nm^2 and 1.44- 1.96 nm^2 respectively if the assumption is made that the lower rim groups make contact with the water surface and the upper rim groups protrude orthogonally from the plane of the surface.

LB: *Π-A isotherm* From the isotherm, the limiting area (A_{lim}) values are slightly different for of the two

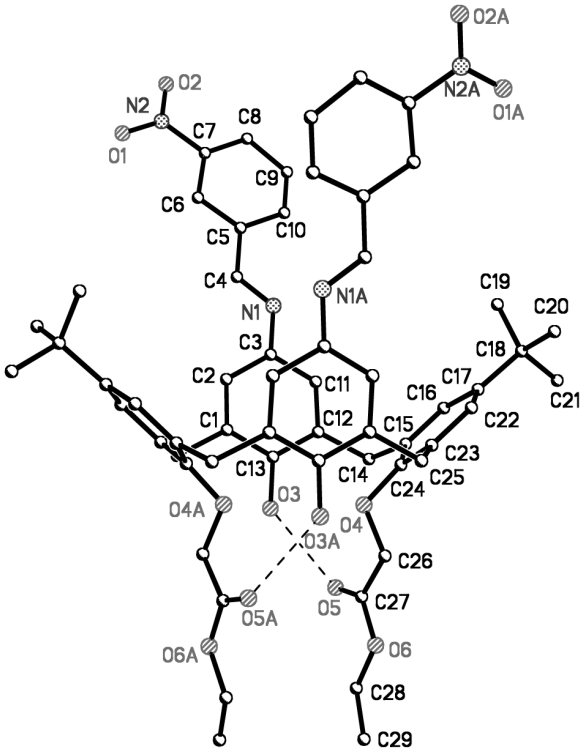

FIGURE 4. Perspective view of Calix-Schiff **II**. Dashed lines represent hydrogen bonds and atoms with the suffix "A" are symmetry equivalents generated by the symmetry transformation -x+1,y,-z. Hydrogen atoms have been omitted for clarity

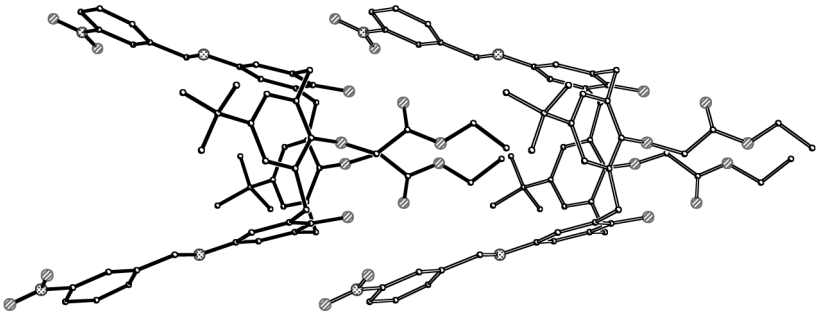

FIGURE 5. Stacking arrangement of II

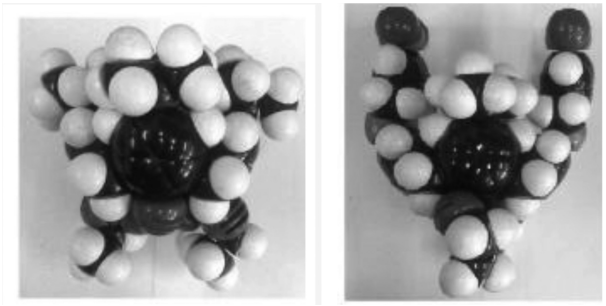

FIGURE 6. CPK modelling for **I** (left) and **II** (right); Front view

calix[4]arene. The limiting area of both films increases upon the additional of Fe^{3+} salt in subphase, indicating that the Fe^{3+} ions have been incorporated into the calixarene layer, most probably within the lower rim region since there would be a strong interaction between the triply charged cation and the oxygen lone electron pairs.

The size for both calix[4]arenes using the CPK modelling ranges from 1.1 nm to maximum 2.5 nm while from the experimental values, A_{lim} (Figure 7), the values are estimated to be around 1.28 nm to 1.40 nm and 1.70 nm to 1.78 nm for **I** and **II** respectively (Table 1). By comparing the modelled values using CPK modelling with the limiting area, conclusion can be drawn that the calixarenes are orientated such that the plane of the calix ring is parallel to the water surface (Lonetti et al. 2005). Figure 8 shows the possible orientations of the calixarene molecules.

SURFACE POTENTIAL (ΔV) AND EFFECTIVE DIPOLE MOMENT OF MOLECULES AT THE INTERFACE ($\mu_\perp$).

Figure 9 depicts the *ΔV-A* versus area per molecule relationship for **II** on a pure water subphase. The relationship can be seen at the onset of the surface potential occurs at slightly larger area for the ion-doped subphase, as is also the maximum $\mu_\perp$ reached. This suggests that the inclusion of the Fe^{3+} ions is contributing to the overall measured potential.

Table 2 presents the individual potential values for both materials along with the effective dipole moments over the Fe^{3+} concentration range studied. These data are

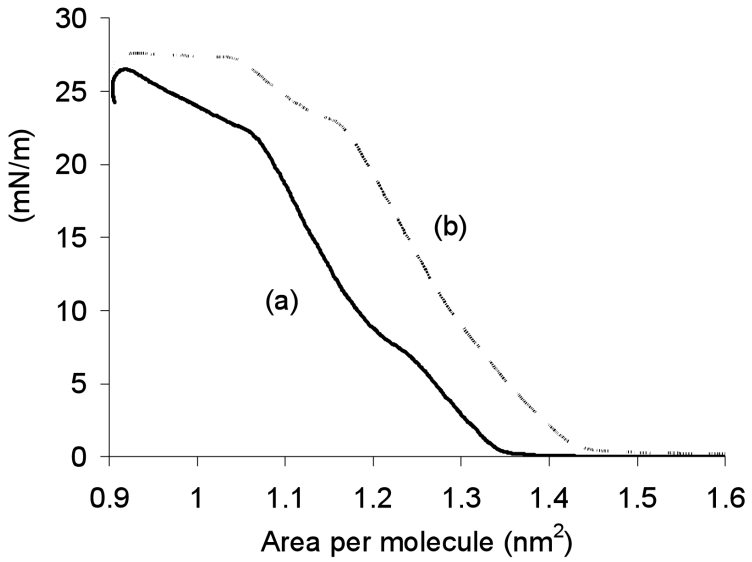

FIGURE 7. Π-A isotherm for **I**; the limiting area increased from (a) water subphase to (b) Fe^{3+} salt (12.50×10^{-2} mM)

TABLE 1. Limiting area and possible orientation of I and II in water subphase and Fe^{3+} subphase

	Subphase	Concentration (1.00×10^{-2} mM)	I		II	
			A_{lim} (nm^2)	Orientation	A_{lim} (nm^2)	Orientation
1	Water	0	1.28	∥	1.70	∥
2	Fe^{3+} salt	1.25	1.30	∥	1.86	∥
3		2.50	1.32	∥	1.71	∥
4		3.75	1.44	∥	1.82	∥
5		5.00	1.32	∥	1.85	∥
6		6.25	1.40	∥	1.80	∥
7		7.50	1.35	∥	1.75	∥
8		8.75	1.36	∥	1.80	∥
9		10.00	1.38	∥	1.70	∥
10		11.25	1.40	∥	1.80	∥
11		12.50	1.40	∥	1.78	∥

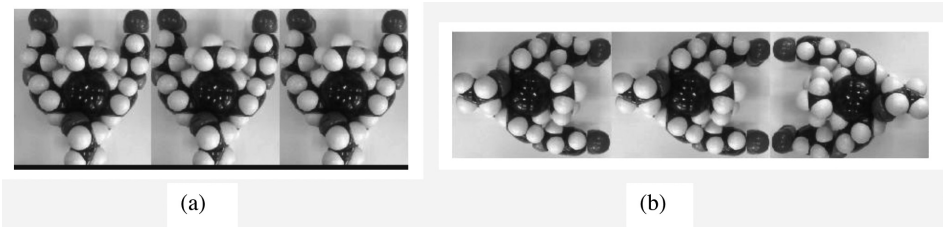

FIGURE 8. Possible orientation of the molecules at water-air interface; (a) parallel orientation (∥), where a line underneath shows where the air/water interface, (b) perpendicular (⊥) orientation.

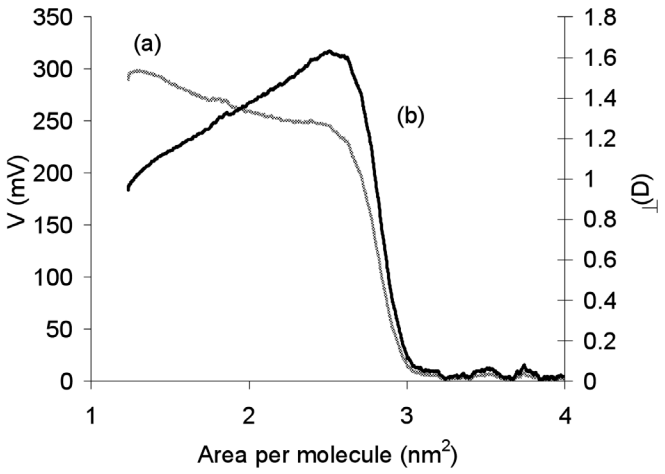

FIGURE 9. (a) Surface potential and (b) effective dipole moment for **II**

plotted in Figure 10 as a function of concentration. For both calixarenes, ΔV gradually rises up to ~0.04 mM, before stabilising for higher concentrations. This suggests that the potential rises monotonically as increasing number of Fe^{3+} ions are incorporated into the calixarene monolayer, but once the maximum amount of ions have been complexed, no further increase in ΔV is possible.

As expected, $\mu_{\perp}$ of the complex (Figure 11) increases rapidly to a maximum value at a concentration of ~0.04 mM (Taylor et al. 1992).

The $\mu_{\perp}$ measured for II is significantly larger than that for I. This is because the presence of the conjugated electron system terminated in the nitro group in **II** compared to the simple methyl group in material **I** lead to a strong dipole that is aligned orthogonally with respect to the plane of the water surface. The $\mu_{\perp}$ calculations have used $\varepsilon = 1$ for both materials; as most researchers assume that for ultra-thin films since the thickness of the air gap between the monolayer and the vibrating electrode is very large compared to the thickness of the monolayer itself.

Conclusion

The Langmuir properties of two calixarenes containing very different upper rims (calixarene **II** whichisa conjugated push-pull electron system, and calixarche **I** which is a small-dipole system) have been investigated. Π-A isotherms and ΔV plots have revealed that Fe^{3+} ions

TABLE 2. Surface potential maximum (ΔV_{max}), and effectife dipole moment of molecules at the interface ($\mu_{\perp}$)

	Subphase	Concentration (1.00×10^{-2} mM)	ΔV_{max} (mV)		$\mu_{\perp max}$ (D)	
			I	**II**	**I**	**II**
1	Water	0	378	244	1.15	1.63
2	Fe^{3+} salt	1.25	410	276	1.50	1.97
3		2.50	418	298	1.54	2.19
4		3.75	425	312	1.68	2.05
5		5.00	426	310	1.53	2.04
6		6.25	412	308	1.60	1.86
7		7.50	432	304	1.66	1.88
8		8.75	425	314	1.73	2.05
9		10.00	432	312	1.72	1.96
10		11.25	430	312	1.78	1.99
11		12.50	425	311	1.77	1.99

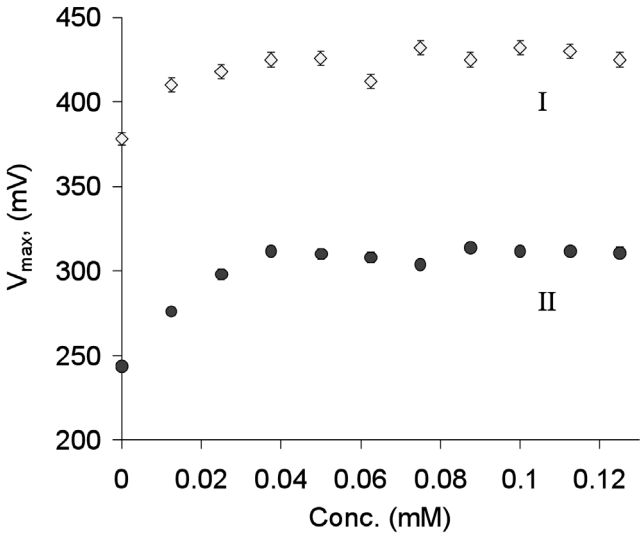

FIGURE 10. Surface potential maximum, ΔV_{max} versus concentration for **I** and **II** added with Fe^{3+} salts

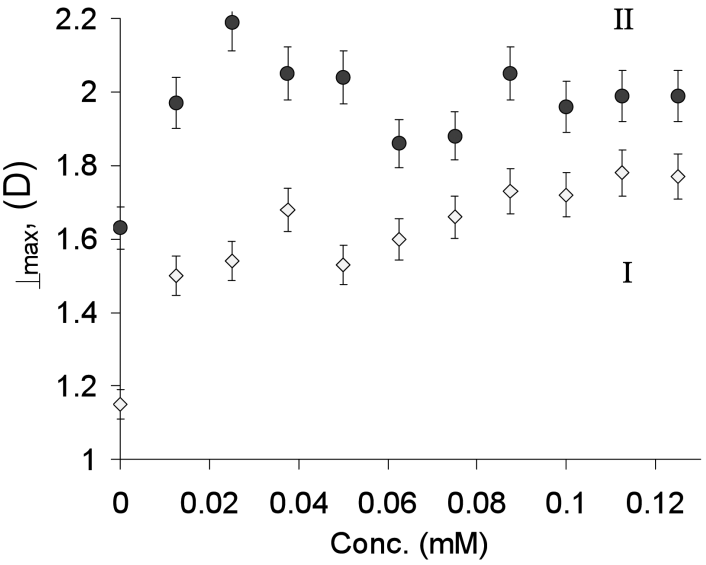

FIGURE 11. Effective dipole moment, $\mu_{\perp \max}$ versus concentration for **I** and **II** added with Fe^{3+} salts

are incorporated into the floating monolayers. The change in ΔV for compressed monolayers of both calixarenes increases monotonically with increasing concentration until saturating at ~0.04 mM, suggesting that the extent of ion uptake has maximised at this concentration. This work implies that the use of ΔV measurements on floating Langmuir films may be useful in monitoring ion concentrations in water over this concentration range. Future work will be aimed at similar ΔV measurements on transferred LB films of these calixarenes in order to identify whether these materials could form the basis of solid state sensors for aqueous ions.

ACKNOWLEDGEMENTS

F.L.S. wishes to acknowledge the Universiti Pendidikan Sultan Idris (UPSI) and Government of Malaysia for the award of a scholarship which enabled her to undertake this work. J.P.W. wishes to thank the Postgraduate R&D Skills Programme, and ITT-Dublin's PhD Continuation Fund for grant support.

Crystallographic data have been deposited with the Cambridge Crystallographic Data Centre as supplementary publication no. CCDC 746610. Copies of the data can be obtained, free of charge, on application to CCDC, 12 Union Road, Cambridge CB2 1EZ, UK (fax: +44-(0)1223-336033 or e-mail: deposit@ccdc.cam.ac.uk).

REFERENCES

Aisen, P. & Wesling-Resnick, E.A. 1999. Iron metabolisme. *Curr. Opin. Biol*. 3: 200-206.

Andrews, N.C. & Engl. N. 1999. Disorder of iron metabolisme. *J. Med*. 341: 1986-1995.

Arnaud-Neu, F., Collins, E.M., Deasy, M., Ferguson, G., Harris, S.J., Kaitner B., Lough, A.J., McKervey, M.A., Marques, E., Ruhl, B.L., Schwing, M.J. & Seward, E.M. 1989. Synthesis, x-ray crystal structures, and cation-binding properties of alkyl calixaryl esters and ketones, a new family of macrocyclic molecular receptors. *J. Am. Chem. Soc*. 111: 8681-91.

Beutler, E., Felitti, V., Gelbart, T. & Ho, N. 2001. Genetics of iron storage and hemochromatosis. *Drug Metab. Dispos*. 29: 495- 499.

Burla, M.C., Caliandro, R., Camalli, M., Carrozzini, B., Cascarano, G.L., Caro, L.D., Giacovazzo, C., Polidori, G. & Spagna, R. 2005. *SIR2004*: an improved tool for crystal structure determination and refinement. *J. Appl. Cryst*. 38: 381- 388.

Cadogan, A., Deasy, M., Diamond, D. McKervey, M. A. 1989. Sodium-selective polymeric membrane electrodes based on calix[4]arene ionophores. *Analyst* 114: 1551-4.

Cairo, G. & Pietrangelo, A. Iron regulatory proteins in pathobiology. 2000. *Biochem. J.,* 352, 241-50.

Casnati, A. & Ungaro, R. 2000. Calixarenes in spherical metal ion recognition, in. *Calixarenes in Action*, edited by L. Mandolini, R. Ungaro: 62-84.

Collins, E.M. & McKervey, M.A. 1989. Molecular receptors with the calix[4]arene substructure. Synthesis of derivatives with mixed ligating functional groups. *J. Chem. Soc. Perkin Trans*. 1: 372-374.

Creaven, B.S., Deasy, M., Flood, P.M., McGinley, J. Murray, B.A. 2008. Novel calixarene- Schiff bases that bind silver(I) ion. *Inorganic Chemistry Communications* 11(10): 1215-1220.

Creaven, B.S., Donlon, D.F. & McGinley, J. 2009. Coordination chemistry of calix[4]arene derivatives with lower rim functionalisation and their applications. *Coordination Chemistry Reviews* 253(7-8): 893-962.

Diamond, D. & McKervey, M.A. 1996. Calixarene-based sensing agents. *Chem. Soc. Rev*. 25: 15-24.

Eisenstein, R.S. 2000. Molecular control of mammalian iron metabolism. *Annu. Rev. Nutr*. 20: 627-662.

Fanucci, G.E., Backov, R., Fu, R. & Talham, D.R. 2001. Multiple Bilayer dipalmitoylphosphatidylserine LB films stabilized with transition metal ions. *Langmuir* 17: 1660- 1665.

Gutsche, C.D. 1998. *Calixarenes Revisited*. J.F. Stoddart. (ed.) Cambridge, UK: The Royal Society of Chemistry.

Gutsche, C.D., Dhawan, B., No, K.H. & Muthukrishman, 1981. Calixarenes 4. The synthesis, characterization, and properties of the calixarenes from P-tert-Butylphenol. *J. Am. Chem. Soc*. 103: 3782-92.

Gutsche, C.D., Levine, J.A., Sujeeth & P.K. Calixarenes. 1985. Functionalized calixarenes: The Claisen rearrangement route. *J. Org. Chem*. 50: 5802-6.

Korchowiec, B., Salem, A.B., Corvis, Y., Regnouf de Vains, J.B., Korchowiec, J. & Rogalska, E. 2007. Calixarenes in a membrane environment: A monolayer study on the miscibility of three p-tert-butylcalix[4]arene β-lactam derivatives with 1,2-dimyristoyl-sn-glycero-3-phosphoethanolamine. *J. Phys. Chem*. 11: 13231-13242.

Langmuir Films or Insoluble Monolayers at the Air Water Interface, http://www.mnp.leeds.ac.uk/sdevans/lectures/lecture%207_8.pdf [15 June 2009].

Lonetti, B., Nostro, P.L., Ninham, B.W. & Baglioni. P. 2005. Anion Effects on Calixarene Monolayers: A Hofmeister Series Study. *Langmuir 21:* 2242-2249.

Lu, J., Chen, R. & He, X. 2002. A lead ion-selective electrode based on a calixarene carboxyphenyl azo derivative. *Electroanal. Chem*. 528, 1-2: 33- 38.

Lu, J.Q., Pang, D.W., Zeng, X.S. & He, X.W. 2004. A new solid-state silver ion-selective electrode based on a novel tweezer-type calixarene derivative. *J. Electroanal. Chem*. 568: 37- 43.

Lu, J., Tong, X. & He, X. 2003. A mercury ion-selective electrode based on a calixarene derivative containing the thiazole azo group. *J. Electroanal. Chem*. 540: 111- 117.

Munch, J. H. & Gutsche, C.D. 1990. p-tert-Butylcalix[8]arene (preparation). *Org. Synth*. 68: 233-6.

Nabok, A.V., Richardson, T., Davis, F. & Stirling, C.J.M. 1997. Cadmium Sulfide Nanoparticles in Langmuir- Blodgett Films of Calixarenes. *Langmuir* 13: 3198-3201.

NIMA Technology, Surface Potential Sensor. http://www.nima.co.uk/surface-potential-sensor.aspx [15 June 2009].

O'Connor, K.M., Svehla, G., Harris, S.J. & McKervey, M.A. 1992. Calixarene-based potentiometric ion- selective electrodes for silver. *Talanta* 39 (11): 1549- 54.

Osvaldo, N.O. & Bonardi, C. 1997. The surface potential of *Langmuir* monolayer revisited. *Langmuir* 13: 5920-5924.

Sheldrick, G.M. 2008. A short history of SHELX. *Acta Cryst*. A64: 112-122.

Schmitt, P., Beer, P.D., Drew, M.G.B. & Sheen, P.D. 1997. Calix[4]tube: A tubular receptor with remarkable pottassium ion selectivity. *Angew. Chem. Int. Ed*. Engl. 36: 1840-1842.

Taylor, D.M. & Bayes, G.F. 1999. The surface potential of Langmuir monolayers. *Material Science and Engineering* C8: 65-71.

Taylor, D.M., Gupta, S.K., Underhill, A.E. & Wainwright, C.E. 1992. Monolayer characterization and multilayer deposition of conducting Langmuir-Blodgett films. *Thin Solid Films* 210/211: 287- 289.

Touati, D. 2000. Iron and oxidative stress in bacteria. *Arch. Biochem. Biophys*. 373: 1- 6.

Verboom, W., Durie, A., Egberink, R.J.M., Asfari, Z. & Reinhoudt, D.N. 1992. Ipso nitration of p-tert-butylcalix[4]arenes. *J. Org. Chem*. 57: 1313- 16.

Wang, F., Liu, Q., Wu, Y. & Ye, B. 2009. Langmuir- Blodgett film of p-tert-butylthiacalix[4]arene modified glassy carbon electrode as voltammetric sensor for the determination of Ag+. *J. Electroanalytical Chem*. 630, 49-54.

Wu, Z., Wu, S. & Liang, Y. 2001. Monolayer behavior and LB film structure of Poly(2-methoxy-5-(n-hexadecyloxy)-p-phenylene vinylene). *Langmuir* 17: 7267-7273.

Zhang, H.M., Fu, W.F., Chi, S.M. & Wang, J. An asymmetric imidazole derivative as potential flurescent chemosensor for Fe3+ in aqueous solution. *J. of Luminescence* 129: 589-594.

Zhang, L., Fan, J. & Peng, X. 2009. X-ray crystallographic and photophysical properties of rhodamine-based chemosensor for Fe3+. *Spectrochimica Acta* Part A 73: 398- 402.

Zeng, X., Weng, L., Chen, L., Leng, X., Zhang, Z. & He, X. 2000. Improved silver ion-selective electrode using novel 1,3-bis(2-benzothiazolyl)thioalkoxy-p-tert-butylcalix[4]arenes. 2000. *Tetrahedron Letters* 41 (25): 4917-4921.

F.L. Supian & T.H. Richardson*
Department of Physics & Astronomy
University of Sheffield
Hounsfield Road, Sheffield (UK) S3 7RH, United Kingdom

M. Deasy, F. Kelleher & J.P. Ward
Department of Science
Institute of Technology Tallaght (ITT Dublin)
Dublin 24, Ireland

V. McKee
Department of Chemistry
Loughborough University
Loughborough
Leicestershire (UK) LE113TU, United Kingdom

*Corresponding author; email: t.richardson@sheffield.ac.uk

Received: 17 July 2009
Accepted: 1 October 2009